Frequency Control in an Autonomous Two-area Hybrid Microgrid using Grasshopper Optimization based Robust PID Controller

Anil Annamraju
Department of Electrical Engineering
NITW
Warangal,India
ani223kumar@gmail.com

Srikanth Nandiraju
Department of Electrical Engineering
NITW
Warangal,India
nvs@nitw.ac.in

***Abstract*— The intermittency in the renewable energy sources output power, along with the system and load perturbations in the standalone multi-microgrid results in large frequency deviations. The traditional PI/PID controller is unable to provide the acceptable performance for the operating conditions as mentioned above. To address this problem, this paper suggests an efficient load frequency controller for the frequency control of a microgrid (MG). In this proposed controller, the parameters of PID controllers are fine-tuned by using grasshopper optimization algorithm (GOA). In the proposed strategy, diesel engine generators (DEGs) and redox flow batteries (RFBs) are responsible for balancing the generation and load in the hybrid microgrid system. The proposed controller is executed on an autonomous 2-area hybrid microgrid test system, under various parametric and systemic disturbances. Finally, the superiority of the proposed controller is alleviated concerning error reduction, settling time and overshoot by comparing with various techniques available in the literature.**

Keywords—frequency control, robust controller, two-area microgrid, RFBs, grasshopper optimization algorithm.

Symbols

$\Delta f_1, \Delta f_2$	Frequency deviation in the area1, area2
M_1, M_2	The inertia of the area1,area2
D_1, D_2	Damping coefficient of the area1,area2
U_{f1}, U_{f2}	Command signal to the governor in area1, area2
$\Delta P_{DEG1}, \Delta P_{DEG2}$	Change in diesel engine generator output in area1,area2
ΔP_{φ}	Solar radiation changes
ΔP_{PV}	Steady-state changes in the solar power output
ΔP_W	Wind power changes
ΔP_{WTG}	Wind turbine generator output
$\frac{1}{R_1}, \frac{1}{R_2}$	Droop characteristics of area1,area2
$\Delta P_{tie,12}$	Tie power deviations between area 1&2
β_1, β_2	Frequency bias factors of area1, area2
T_1, T_2	DEG speed governor time constants
T_3	Diesel engine time constant
ΔY	Change in the valve position
ΔP_{RFB}	Change in the output power of the RFB
K_{RFB}	Droop gain of RFB
T_{di}	Conversion delay time constant
$X_{i,k}$	Position of i^{th} grasshopper in j^{th} iteration
N_{pop}	Population Size
S_i	Social interaction of the i^{th} grasshopper
G_i	i^{th} grasshopper Gravity force
A_i	Wind deviation
r_1, r_2, r_3	Random numbers between 0 - 1
D_{ij}	The distance between the i^{th} and j^{th} grasshopper
$\widehat{D_{ij}}$	Unit vector from the i^{th} and j^{th} grasshopper
G	Gravity constant
u	Drift constant
$\widehat{e_w}$, $\widehat{e_g}$	Unit vector in the direction of the wind & ground
A	Adaptation factor
A_{min}, A_{max}	Acceleration factor min and max limits
d	Search dimension
$\widehat{T_d}$	Value of the d^{th} dimension in the target
T_{sim}	Simulation time
K_P, K_I, K_D	Gains of the proportional, integral and derivative controllers

I. INTRODUCTION

The increasing need for electrical energy to remote locations like islands & rural areas from the main grid is becoming complicated, costly and environmentally hazardous. An autonomous microgrid (MG) is a reliable and efficient solution for such problems. Many countries like China, South Africa, Japan, et al. installed MGs successfully for providing electrical energy to the remote locations [1-2]. The MG, which comprises various RES and energy storage systems (ESSs) drags the considerable attention of various companies and researchers. Due to uncertainty in the RES output, the importance of various ESSs in MG is justified by several authors[3-5].

Due to intermittency in the RES output power, low system inertia along with significant changes in the load, MG experiences the large frequency deviations and loses its stability. The above factors reveal that MG frequency control

in autonomous mode is difficult than in grid-connected mode [6]. Therefore, the MG requires efficient and intelligent controllers to control the frequency within the tolerable limits.

Similar to conventional power sources, LFC for MG is done with various control levels are proposed by several authors [7-20].In [7-10], the authors proposed various ESSs based approaches for primary frequency control of MG. In this primary level, DEG droop settings try to arrest the frequency deviations at the initial stage, but it doesn't stabilize the system to a new set point. For this, a supplementary control action is required which is known as secondary frequency control (SFC).

The typical control strategy for the SFC problem is injecting a restorative signal to governor summing point using fixed gain PI/PID controllers[11]. However, conventional controller fails to keep frequency variations within acceptable limits because of high nonlinear nature of various sources, loads and with low system inertia. From past few years, several researchers proposed various meta-heuristic techniques to optimize the PID controller of the MG. In [6&12], the authors proposed μ synthesis & H-∞based frequency controllers for MG frequency control. Besides, several authors proposed with various soft computing techniques for the frequency control of MG such as ANN based controller[13], fuzzy logic based controllers[14-16]. In[17-25], the authors proposed various meta-heuristic techniques to tune the parameters of the PID controller for the frequency control of MG. In[17] GA based technique, in [18] BBO technique, in [19] QOHS technique, in [20] GWO technique, in [21] SSO technique etc.

In previous techniques[17,19,21], authors incorporated individual controllers for each source (i.e., for diesel engine generator, fuel cell, battery etc). The drawback of this is the number of variables to optimize is increasing. In this paper, an efficient, coordinated strategy is proposed between diesel engine generators (DEGs) and redox flow batteries(RFBs) to reduce the frequency deviations in the MG. The first application of grasshopper optimization (GOA) was developed to tune the PID controller parameters. The primary goal of this work is to demonstrate the efficiency and robustness of the suggested GOA optimized PID controller in an autonomous MG with all possible uncertainties (i.e., load changes, renewable power uncertainties and parametric uncertainties). Finally, simulation results are compared with some recent and standard optimization techniques available in the literature.

II. MODELLING OF TWO-AREA HYBRID MG

Fig.1 shows the linearized model of the two-area autonomous hybrid MG, which comprises of DEG, RFB, WTG, PV, and Load[14,21]. The necessary MG parameters for simulation are given in the appendix. The detailed modeling of each component is explained in the subsequent sections.

The frequency deviations in each area of MG can be expressed as:

$$\Delta f_1 = \frac{1}{M_1 s + D_1}(\Delta P_{DEG1} + \Delta P_{WF} - \Delta P_{RFB} - \beta_1 \Delta f_1 - \Delta P_{L1})$$
$$\Delta f_2 = \frac{1}{M_2 s + D_2}(\Delta P_{DEG2} + \Delta P_{PV} - \Delta P_{RFB} - \beta_2 \Delta f_2 - \Delta P_{L2}) \quad (1)$$

Where, $\Delta P_{tie,12}$ is defined as:

$$\Delta P_{tie,12} = \frac{T_{12}}{s}(\Delta f_1 - \Delta f_2) \text{ and } \Delta P_{tie,21} = -\Delta P_{tie,12} \quad (2)$$

In the interconnected MG, the objective is to restore the generation-load balance in each area by minimizing the area control error (ACE) to tolerable limits (ideally ACE=0). The ACE of each area is defined as:

$$ACE_1 = \Delta f_1 + \Delta P_{tie,12}$$
$$ACE_2 = \Delta f_2 + \Delta P_{tie,21} \quad (3)$$

Finally, the controller output applied to the governor for power balance is expressed as:

$$U_{fi} = K_p ACE_i + \frac{K_I}{s} ACE_i + K_D * (sACE_i) \text{ where i=1,2} \quad (4)$$

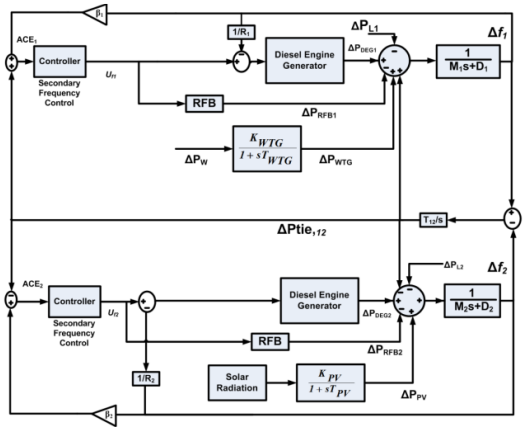

Fig. 1 Block diagram of two area model

A. DEG modeling

DEG is responsible to maintain the generation-load balance in an MG, by supplying the deficient power to the load based on RES output.Fig.2 depicts the linearized model of DEG [22]. Speed governor adjusts the valve position based on the command signal (U_f) from the controller, ΔY is the change in the valve position.

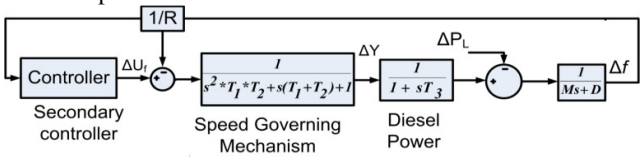

Fig.2 Block diagram of DEG model

B. Wind turbine generator (WTG) modelling

The WTG output power depends upon the wind speed, which is random by nature. The mechanical power output of the windmill (P_w) is expressed as[23]:

$$P_w = \frac{1}{2} C_p(\lambda, \beta) \rho V_w^3 A \quad (5)$$

here 'ρ' is air density, 'V_w' is the wind velocity, 'A' is swept the area, 'C_p' is power coefficient The C_p can be expressed as[23]:

$$C_p(\lambda, \beta) = 0.22\left(\frac{116}{\gamma} - 5 - 0.4\beta\right) exp^{-125/\gamma}$$

$$\gamma = [\frac{1}{\lambda + 0.08\beta} - \frac{0.035}{1+\beta^3}]^{-1}$$
$$\lambda = \frac{R\omega}{V_\omega} \quad (9)$$

In this work GAMESA company WTG is used [25].In this study, windmill output power (P_W) data is collected at different wind speeds(V_w) and, by using curve fitting technique an equation for output power of windmill is developed in terms of wind speed(V_w).The output power of WTG (P_W) can be expressed as[25]:

$$P_W = \begin{cases} P_{rated}, & V_{rated} \le V_w \le V_{cutout} \\ 0, & V_{cutin} \le V_w \le V_{rated} \\ 0.0013V_w^6 - 0.046V_w^5 + 0.33V_w^4 + 3.68V_w^3 - 51V_w^2 + 2.33V_w + 366, & else \end{cases} \quad (10)$$

Here, the small signal stability analysis is to be performed. So, a change in wind power ((ΔP_W)) is needed.The ΔP_W is obtained by differentiating Eq.(10), which is expressed as:

$$\Delta P_W = \begin{cases} 0, & V_{rated} \le V_w \le V_{cutout} \\ 0, & V_{cutin} \le V_w \le V_{rated} \\ 0.0078V_w^5 - 0.23V_w^4 + 1.32V_w^3 + 11.04V_w^2 - 102V_w + 2.33, & else \end{cases} \quad (11)$$

Finally, to accommodate the all conversion delays in the WTG a first order transport delay is introduced in the system. Finally, the WTG output power can be expressed as[14]:

$$\frac{\Delta P_{WTG}}{\Delta P_w} = \frac{1}{1+sT_{WTG}} \quad (12)$$

C. PV model

PV array consists of multiple modules in parallel and series combination. The number of modules in parallel and series depends on the required current and voltage of the array. The voltage to the current relation in PV system is nonlinear. The PV array output power varies due to either change in load current (or) solar radiation. For this frequency regulation study, it is considered that the PV power varies only due to solar radiations. The mathematical model of PV array is expressed as[14]:

$$TF_{PV} = \frac{\Delta P_{PV}}{\Delta P_\varphi} = \frac{1}{1+sT_{PV}} \quad (13)$$

D. Redox Flow Batteries (RFB) modeling

Conventional frequency regulation units like DEG responds slowly for frequency deviations. The slow action is due to large time constants involves in the DEG response. For abrupt changes in the RES output and load, the DEG may not accommodate the changes rapidly[6]. To overcome this, an efficient ESS is needed, and RFB is the most suitable one for such a scenario. The RFBs have the advantage of fast-acting capability, easy maintenance and recharge ability compared to other ESSs [25]. Fig.3 depicts the transfer function model of RFB [20].The expression for the instantaneous change in RFB power according to controller command can be expressed as:

$$\Delta P_{RFB} = \left(\left[U_f * K_{RFB}\right] - \left[\frac{K_{ri}}{1+sT_{ri}}\right]\right) * \left(\frac{1}{1+sT_{di}}\right) \text{ - set value} \quad (14)$$

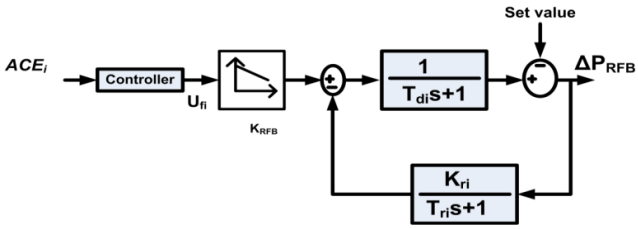

Fig.3 The control structure of RFB

III. TUNING OF PID CONTROLLER THROUGH GOA

In recent years, nature-inspired heuristic optimization algorithms have become more popular in solving complex mathematical and engineering problems. Many of these algorithms are derived from the swarm behavior occurring in nature. One such recent algorithm, which mimics the nature of swarm of grasshoppers is grasshopper optimization algorithm developed by mirjali et al. in 2017 [26].

Grasshoppers are considered as pests since they possess a threat to farming crops and agriculture. They mostly love individual lives but join in to form large swarms to eat away the crops and cause devastation. The swarm size may be of a mainland scale and a nightmare for farmers. Grasshoppers show swarm behavior in 2 stages of their life. First in the nymph stage and then in adulthood. In nymph stage millions of nymphs join together, jump and roll like cylinders to move. While in adulthood they develop wings. So they can fly in the air as well as jump at longer distances than in the nymph stage. In bio-inspired algorithms, the search process is divided mainly into exploration and exploitation. In the first stage, the search agents are encouraged to move abruptly, and in the second stage, they tend to move locally in the search space. The grasshopper swarms in the adulthood move abruptly over vast distances by flying leading to exploration characteristic. While in nymph mode they move slowly with small steps leading to exploitation of search space. All these while seeking the food source which is the primary requirement. This behavior is used to make a mathematical model shown as follows:

Like all heuristic techniques, the initialization of the population for the first iteration as follows:

$$X_{i,0} = lb + randomno(1, N_{pop}) * (ub - lb) \quad (15)$$

For the next iteration, the position of the i^{th} particle in the k^{th} iteration is modified based on the equation [27]:

$$X_{i,k} = r_1 S_i + r_2 G_i + r_3 A_i \quad (16)$$

Where,

$$S_i = \sum_{j=1,\neq i}^{Npop} s(D_{ij}).\widehat{D_{ij}} \quad (17)$$

The s function denotes the social forces, which can be calculated as [27,28] :

$$s(D_{ij}) = 0.5e^{-D_{ij}}\left(e^{-\frac{2}{3}} - 1\right); G_i = -G.\widehat{e_g}; A_i = u.\widehat{e_w}; \widehat{D_{ij}} = \frac{X_i - X_j}{D_{ij}} \quad (18)$$

To maintain the balance between exploitation and exploration an adaptation factor (A) is introduced as follows :

$$A = A_{max} - k.\frac{A_{max}-A_{min}}{\text{Max\_Iter}} \quad (19)$$

A modified version of A –factor to solve optimization problems is given as:

$$A_i^d = A\left(\sum_{i=1,j\neq i}^{Npop} A.\frac{ub_d-lb_d}{2}.s(D_{ij}).\widehat{D_{ij}}\right) + \widehat{T_d} \quad (20)$$

The GOA technique was tested with 30 benchmark functions, and supremacy of GOA is exhibited by comparing with some standard and powerful techniques available in the literature such as GA, DE, PSO, FA, CS, FPA, SMS, BFO[28]. Due to its tremendous merits such as simplicity, easy implementation structure, less number of controlling parameters compared to other techniques and fast convergence characteristics, GOA technique applied successfully to various fields of engineering problems[26-28]. By accounting all these advantages, in this work, GOA technique is opted to optimize the PID controller.

The objective of LFC is to keep frequency deviation and power tie line deviations minimum or zero. Hence, integral-of-the-time absolute error (ITAE) is selected as fitness function(FF). which is to be minimized with the help of PID gains as variables

$$\text{Minimize}(FF) = Min\left\{\int_0^{T_{Sim}} t.\left(|\Delta f_1| + |\Delta f_2| + |\Delta P_{tie,12}|\right).dt\right\} \quad (21)$$

Subjected to limits of PID gains as:

$$K_{p,i,d}^{min} \leq K_{p,i,d} \leq K_{p,i,d}^{max} \quad (22)$$

IV. RESULTS AND DISCUSSIONS

In order to demonstrate the effectiveness of suggested control strategy, a time-domain simulations are carried out with the test system as shown in the Fig.1 by using MATLAB/SIMULINK software. A comparative study of four controllers i.e. GOA tuned PID controller, SSO tuned PID controller, GA tuned PID controller & classical PID controller are carried out in presence of ΔP_L, ΔP_{WP}, ΔP_φ as disturbances. Finally, superiority and robustness of the GOA tuned PID controller is demonstrated under various scenarios.

Scenario 1

In this scenario, the only single area is considered. The primary aim of this scenario is to show how the conventional PID controller fail to stabilize the frequency deviations when all possible uncertainties (i.e., ΔPL, ΔPWP, ΔPφ) happens concurrently. Fig.4 shows the frequency deviations in a single area with three controllers.

From this scenario, it is clear that the conventional PID controller fails to stabilize the frequency deviations when all uncertainties happen simultaneously. However, rest of the controllers providing the acceptable performance hence, these controllers are considered as robust controllers.

Scenario 2

In this scenario, a step load disturbance of 0.1 p.u is considered at t=5 seconds in the area1.The frequency deviations in the two areas and tie-line power flow deviations are shown in Fig.5 (a),(b) & (c).The ITAE of the inter-connected system with various techniques for scenario 2 are given in Table 1.

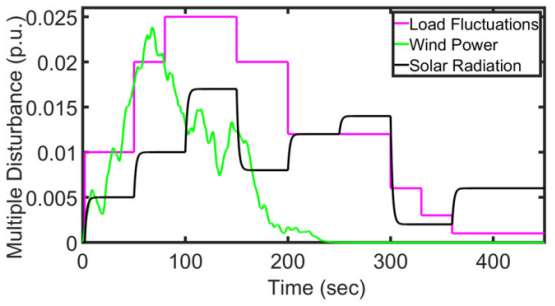

(a)

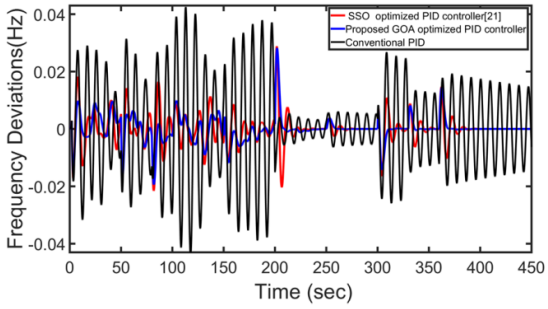

(b)

Fig.4 (a) multiple disturbances in MG (b) frequency deviations in MG with the single area alone

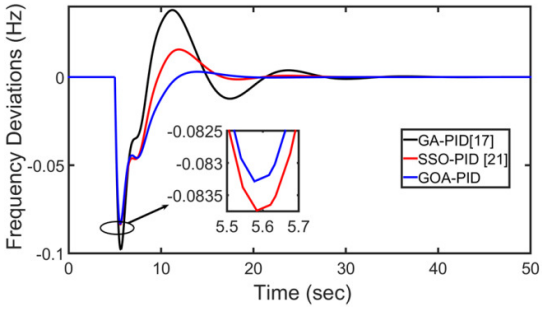

(a)

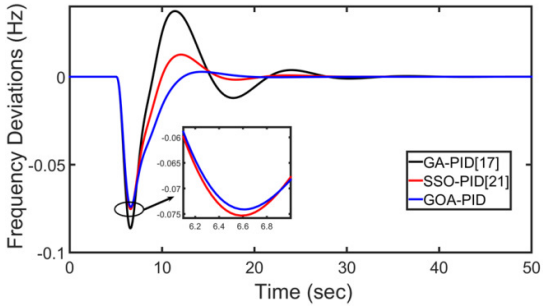

(b)

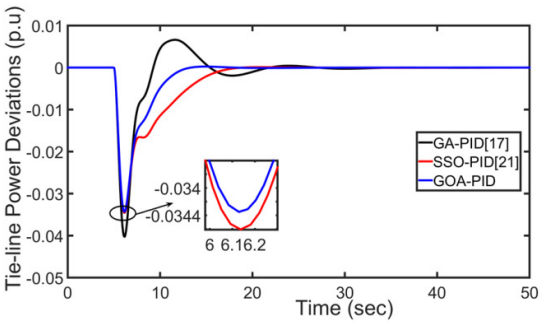

(c)

Fig.5 a), b) frequency deviations in area1 & 2 c)tie-line power flow deviation

Table 1 Performance indices with various controllers in two-area MG

Methods	Performance indices					
	Area 1		Area 2		Tie-line power deviation	
	Peak Undershoot (Hz)	Settling Time (sec)	Peak Undershoot (Hz)	Settling Time (sec)	Peak Undershoot (MW)	Settling Time (sec)
GA-PID [17]	0.09875	33	0.0865	33.5	0.0403	26
SSO-PID [21]	0.084	24.5	0.076	27	0.0346	18
GOA-PID	0.0832	19	0.0741	20	0.0342	13

The optimal gains of the PID controller with various optimization techniques are given in Table2.

Table 2 Optimized PID parameters with various controllers

Methods	Optimized PID parameters (Area1)			Optimized PID parameters (Area2)		
	K_P	K_I	K_D	K_P	K_I	K_D
GA-PID [17]	3.231	2.4032	5	2.7613	0.3081	3.5061
SSO-PID [21]	4.7781	0.9741	3.60	3.0540	0.5877	2.9625
GOA-PID	4.9	0.844	2.99	0.7189	0.09	4.5494

From the results, it is evident that proposed GOA-PID controller improves the dynamic response of the system effectively compared to GA-PID & SSO-PID. Form this scenario, it is clear that SSO-PID controller providing better response compared to GA-PID controller.To get a better view of results, best of two in three controllers i.e. GOA-PID, SSO-PID controllers are considered for the next scenario.

Scenario 3

The aim of this scenario is to show the robustness of proposed controller with parametric uncertainties [40 % reduction in H & D] along with multiple step loads and random wind power changes in area-1, solar power changes in area-2.The load disturbances, wind and solar power changes are taken as shown in Fig.4(a). The corresponding frequency deviations in area 1, area 2 and tie-line power deviations are shown in Fig.6 (d),(e) & (f). The ITAE performance index for different scenarios with four controllers are given in Table 3.

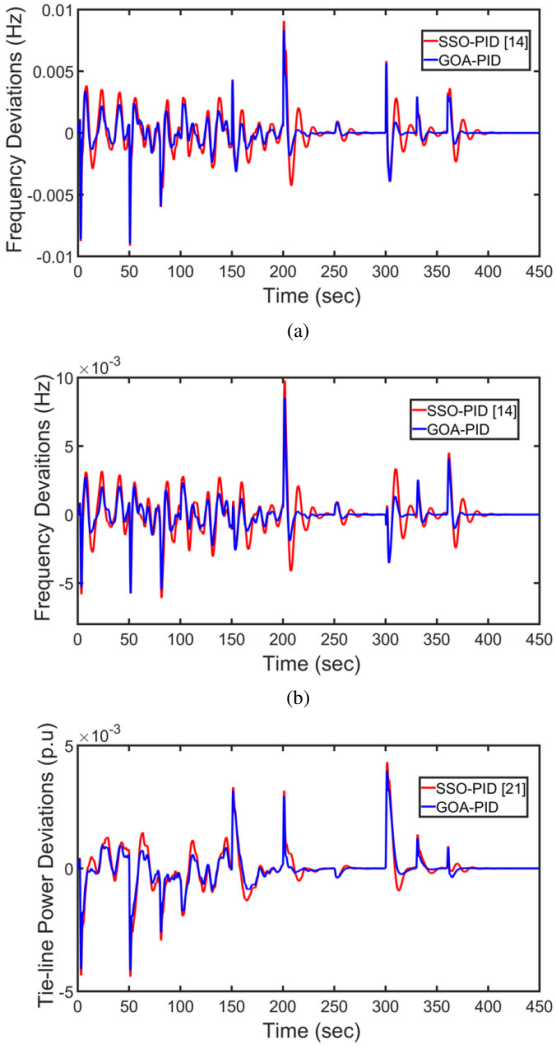

Fig.6 (a), (b) frequency deviations in area-1 & area-2, (c) tie-line power flow deviations between area-1 & area-2

Table 3 Performance index for different scenarios

Scenario	Conventional PID	GA-PID [17]	SSO-PID [21]	GOA-PID
Scenario 1	Unstable	0.000563	0.000471	0.000396
Scenario 2	1.2*10^-4	6.2*10^-5	5.15*10^-5	4.9*10^-5
Scenario 3	Unstable	0.00158	0.00103	0.000962

From the three scenarios, simulation results reveal that the proposed GOA-PID controller is providing superior performance than other two controllers. Diversity in load, high uncertainty in renewable generation and complexity in functionality makes frequency control of autonomous MG is more complex. As shown in the results, the conventional controller fails to meet frequency limitations. From the above

results, it is evident that the robust frequency controller like proposed GOA-PID may be an inevitable solution for MGs and it may also be suitable for modern power grids.

V. CONCLUSION

In this paper, the first application of GOA technique is attempted to tune the parameters of the PID controller for frequency control of an MG. In practice, classical PID controller unable to provide the stable performance in the presence of multi uncertainties. With concern to this, the GOA-PID controller is tuned in a way to reduce the frequency deviations as much as possible. Three critical scenarios are considered to highlight the superiority and robustness of the proposed controller. From the results, it is evident that the proposed strategy improved the system response concerning error reduction, settling time and overshoot in comparison with the other methods available in the literature.

Appendix

MG Parameters

M_1,M_2=0.1667,D_1,D_2(puMW/s)=0.01,β_1,β_2(puMW/s)=0.4216,

R_1,R_2(Hz/puMW)=2.4,K_{WTG},K_{PV}=1,T_1(sec)=0.025,T_2(sec)=2,T_3(sec)=3,

T_{WTG}(sec)=2, T_{PV}(sec)=1.5, T_{12} (puMW)=0.707.

RFB Parameters

$K_{RFB} = 0.5, T_d(sec)$=0.05, $T_r(sec) = 1.8, K_r = 1$

REFERENCES

[1] "IEEE Guide for Design, Operation, and Integration of Distributed Resource Island Systems with Electric Power Systems," in *IEEE Std 1547.4-2011* , pp.1-54, 20 July 2011.

[2] J. Dekker, M. Nthontho, S. Chowdhury, and S. P. Chowdhury, "Economic analysis of PV/diesel hybrid power systems in different climatic zones of South Africa," *Int. J. Electr. Power Energy Syst.*, vol. 40, no. 1, pp. 104–112, Sep. 2012.

[3] D. Lee and L. Wang, "Small-Signal Stability Analysis of an Autonomous Hybrid Renewable Energy Power Generation/Energy Storage System Part I: Time-Domain Simulations," *IEEE Trans. Energy Convers.*, vol. 23, no. 1, pp. 311–320, 2008.

[4] A. Cansiz, C. Faydaci, M. T. Qureshi, O. Usta, and D. T. McGuiness, "Integration of a SMES–Battery-Based Hybrid Energy Storage System into Microgrids," *J. Supercond. Nov. Magn.*, vol. 31, no. 5, pp. 1449–1457, 2018.

[5] K. V Vidyanandan and N. Senroy, "Frequency regulation in a wind–diesel powered microgrid using flywheels and fuel cells," *IET Gener. Transm. Distrib.*, vol. 10, no. 3, pp. 780–788, 2016.

[6] H. Bevrani, M. R. Feizi and S. Ataee, "Robust Frequency Control in an Islanded Microgrid: H_∞ and μ Synthesis Approaches," in *IEEE Transactions on Smart Grid*, vol. 7, no. 2, pp. 706-717, March 2016

[7] J. Li *et al.*, "A Novel use of the Hybrid Energy Storage System for Primary Frequency Control in a Microgrid," *Energy Procedia*, vol. 103, pp. 82–87,Dec 2016.

[8] J. Li, R. Xiong, Q. Yang, F. Liang, M. Zhang, and W. Yuan, "Design/test of a hybrid energy storage system for primary frequency control using a dynamic droop method in an isolated microgrid power system," *Appl. Energy*, vol. 201, pp. 257–269, Sep. 2017.

[9] J. Pahasa and I. Ngamroo, "Coordinated Control of Wind Turbine Blade Pitch Angle and PHEVs Using MPCs for Load Frequency Control of Microgrid," *IEEE Syst. J.*, vol. 10, no. 1, pp. 97–105, 2016.

[10] L. Chen *et al.*, "SMES-Battery Energy Storage System for the Stabilization of a Photovoltaic-Based Microgrid," *IEEE Trans. Appl. Supercond.*, vol. 28, no. 4, pp. 1–7, 2018.

[11] P. K. Ray, S. R. Mohanty, and N. Kishor, "Proportional–integral controller based small-signal analysis of hybrid distributed generation systems," *Energy Convers. Manag.*, vol. 52, no. 4, pp. 1943–1954, 2011.

[12] S. K. Pandey, S. R. Mohanty, N. Kishor, and J. P. S. Catalão, "Frequency regulation in hybrid power systems using particle swarm optimization and linear matrix inequalities based robust controller design," *Int. J. Electr. Power Energy Syst.*, vol. 63, pp. 887–900, 2014.

[13] M. Karimi, H. Mohamad, H. Mokhlis, and A. H. A. Bakar, "Under-Frequency Load Shedding scheme for islanded distribution network connected with mini hydro," *Int. J. Electr. Power Energy Syst.*, vol. 42, no. 1, pp. 127–138, 2012.

[14] A. Annamraju and S. Nandiraju, "Robust Frequency Control in an Autonomous Microgrid: A Two-Stage Adaptive Fuzzy Approach," *Electr. Power Components Syst.*, vol. 46, no. 1, pp. 83–94, Jan. 2018.

[15] N. Govardhan and R. Santhi, " Design of fuzzy PI load frequency controller for hybrid wind diesel system with SMES unit, " Int. Res. J. Eng. Technol., vol. 2. no. 4, pp. 167–174, 2015.

[16] Tarkeshwar and V. Mukherjee, "A novel quasi-oppositional harmony search algorithm and fuzzy logic controller for frequency stabilization of an isolated hybrid power system," *Int. J. Electr. Power Energy Syst.*, vol. 66, pp. 247–261, 2015.

[17] D. C. Das, A. K. Roy, and N. Sinha, "GA based frequency controller for solar thermal–diesel–wind hybrid energy generation/energy storage system," *Int. J. Electr. Power Energy Syst.*, vol. 43, no. 1, pp. 262–279, 2012.

[18] R. H. Kumar and S. Ushakumari, "Biogeography based tuning of PID controllers for Load Frequency Control in microgrid," in *2014 International Conference on Circuits, Power and Computing Technologies [ICCPCT-2014]*, pp. 797–802, 2014.

[19] G. Shankar and V. Mukherjee, "Load frequency control of an autonomous hybrid power system by quasi-oppositional harmony search algorithm," *Int. J. Electr. Power Energy Syst.*, vol. 78, pp. 715–734, 2016.

[20] N. E. Y. Kouba, M. Menaa, M. Hasni, and M. Boudour, "LFC enhancement concerning large wind power integration using new optimised PID controller and RFBs," *IET Gener. Transm. Distrib.*, vol. 10, no. 16, pp. 4065–4077, 2016.

[21] A. A. El-Fergany and M. A. El-Hameed, "Efficient frequency controllers for autonomous two-area hybrid microgrid system using social-spider optimiser," *IET Gener. Transm. Distrib.*, vol. 11, no. 3, pp. 637–648, 2017.

[22] S. A. Papathanassiou and M. P. Papadopoulos, "Dynamic characteristics of autonomous wind–diesel systems," *Renew. Energy*, vol. 23, no. 2, pp. 293–311, 2001.

[23] H. M. Hasanien, "A Set-Membership Affine Projection Algorithm-Based Adaptive-Controlled SMES Units for Wind Farms Output Power Smoothing," *IEEE Trans. Sustain. Energy*, vol. 5, no. 4, pp. 1226–1233, 2014.

[24] WINDPOWER,Availableathttp://www.thewindpower.net/turbine_en_42_gamesa_g52-850.php

[25] D. Lakshmi *et al.*, "Two-area load frequency control using intelligent algorithms in a restructured scenario," *Turk J. Elec Eng & Comp Sci*, vol. 26, no. 2, pp.330-346,2018.

[26] S. Saremi, S. Mirjalili, and A. Lewis, "Grasshopper Optimisation Algorithm: Theory and application," *Adv. Eng. Softw.*, vol. 105, pp. 30–47, 2017.

[27] A. A. El-Fergany, "Electrical characterisation of proton exchange membrane fuel cells stack using grasshopper optimiser," *IET Renew. Power Gener.*, vol. 12, no. 1, pp. 9–17, 2018.

[28] M. Mafarja *et al.*, "Evolutionary Population Dynamics and Grasshopper Optimization approaches for feature selection problems," *Knowledge-Based Syst.*, vol. 145, pp. 25–45, 2018.